THE EFFECT OF STAGE ON FLOW AND COMPONENTS OF THE LOCAL FORCE BALANCE

PETER J. WHITING

Department of Geological Sciences, Case Western Reserve University, Cleveland, OH 44106, U.S.A.

Received 3 April 1995; Revised 4 March 1996; Accepted 25 April 1996

ABSTRACT

Flow fields and water and bed surface topography were measured at two different stages as flow shoals over a submerged mid-channel bar in a straight reach downstream of a bend in Solfatara Creek, Wyoming. The data allow calculation and comparison of the magnitude of the component terms in the downstream and cross-stream force balance at the different stages. At the lower stage, corresponding to a discharge that is 30 per cent of the bankfull discharge, the convective acceleration terms in the equations describing the force balance are important, particularly the terms associated with the cross-stream transport of momentum. These terms are large because of the large accelerations and cross-stream flow forced by the shallow flow over the bar. At the higher stage, corresponding to a discharge that is 45 per cent of the bankfull discharge, flow is more directly downstream and cross-stream velocity is generally less in most of the channel. Downstream flow velocities at the higher stage are larger, but the acceleration is more gradual. Consequently, the convective accelerations at the higher stage tend to be less important than at the lower stage. Results from the two different stages suggest that some of the difference in conclusions reached by various workers on the significance of the various terms in the governing equations may be associated with the relative depth of flow. © 1997 by John Wiley & Sons, Ltd.

Earth surf. processes landf., **22,** 517–530 (1997)
No. of figures: 10 No. of tables: 0 No. of refs: 12
KEY WORDS: channel topography; stage; force balance; boundary shear stress

INTRODUCTION

A number of papers have examined the relative magnitude and importance of the various components of the downstream and cross-stream force balance in channels (Engelund, 1974; Dietrich and Smith, 1983; Odgaard and Bergs, 1988; Whiting and Dietrich, 1991). It is very important for the modelling of channel flow that the appropriate terms in the governing equations be included, otherwise the formulations risk the probability of ignoring critical features of the flow and boundary shear stress fields. These concerns are particularly strong when the bed is mobile and topography adjusts to these boundary shear stress fields.

Workers have disagreed on the importance of the various terms in the governing equations. The differing conclusions may stem from differing channel geometry, the presence of bed and bar forms, whether banks were smooth or rough (flume versus natural channel) and other factors. Some of the difference in conclusions reached by workers may stem from the relative stage of flow during analysis.

To my knowledge, there are no descriptions of the effect of stage on the force balance in channels. In fact, studies of the effect of stage change on flow patterns are themselves rare. Jackson (1975) presented the flow fields at different discharges at a single section in a bend. Dietrich *et al*. (1984) examined the topographic and shear stress pattern adjustments associated with different flows in Muddy Creek, Wyoming, one at about 30 per cent of bankfull and the other at 70 per cent of bankfull. At Muddy Creek the bed was mobile and adjusted rapidly such that flow was in equilibrium with the channel bed. Bridge and Gabel (1992) examined patterns of flow around an emergent mid-channel at various stages. Rhoads and Kenworthy (1995) measured the effect of stage on the downstream and cross-stream flow patterns at stream confluences.

* Contract grant sponsor: Donors of the Petroleum Research Fund (American Chemical Society); Contract grant number: ACS-PRF-18427-AC2

CCC 0197-9337/97/060517–14 $17.50

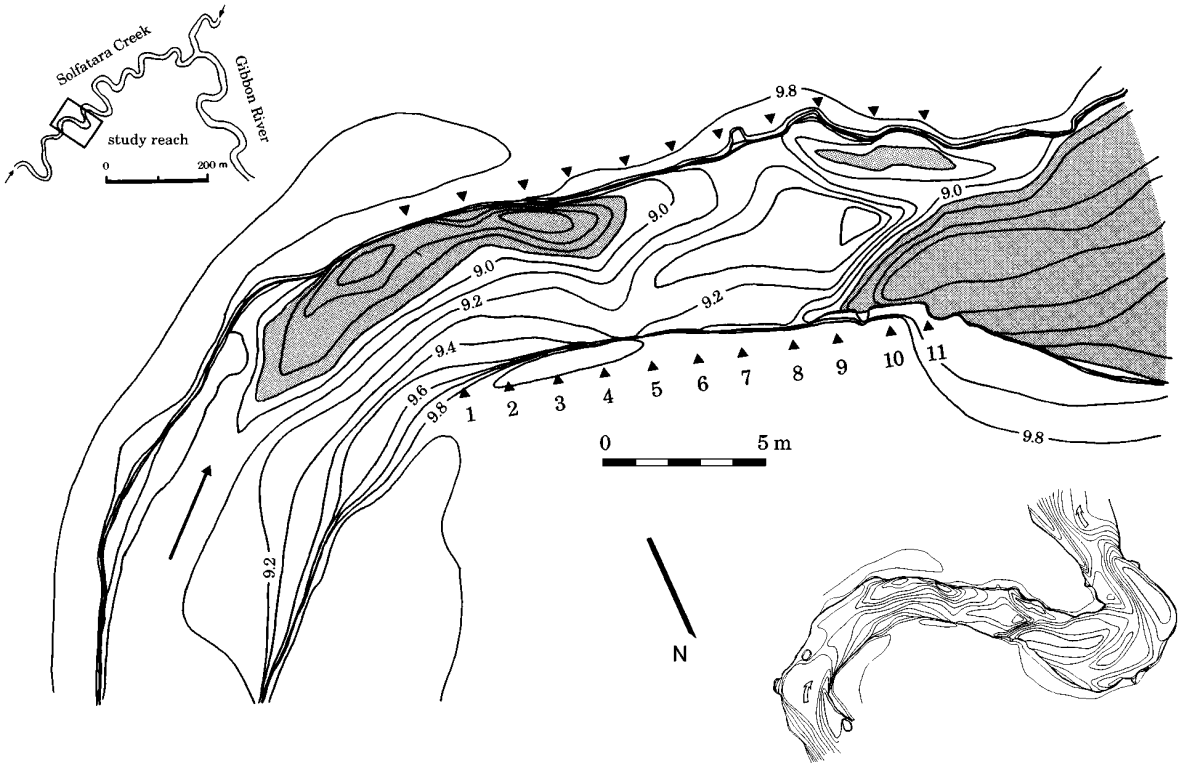

Figure 1. Topographic map of Solfatara Creek in the study area. Flow was measured near section 6 at a water surface elevation of *c.* 9·59 m. Triangles indicate the ends of sections. The shading shows areas below 8·8 m in elevation

Whiting and Dietrich (1991) examined the magnitude of various terms in the equations for the downstream and cross-stream force balance as flow shoaled over a submerged mid-channel bar in Solfatara Creek, Wyoming. These results were for a stage whose discharge was 30 per cent of the estimated bankfull discharge. Another data set was collected at a higher stage whose discharge was 45 per cent of the estimated bankfull discharge. This data set is not quite as complete as that for the lower discharge, but nonetheless is complete enough to draw some original conclusions regarding the relative importance of various terms in the force balances as the bar is progressively submerged. Furthermore, the additional information permits a comparison of the flow and components of the force balance at different stages.

FIELD SITE

Solfatara Creek is a sinuous, gravel-bed channel that averages 5·2 m in width and 0·7 m in depth at bankfull, and has a water surface slope of approximately 0·0010 (Figure 1). Solfatara Creek is located near Norris Junction in Yellowstone National Park, Wyoming, USA, and drains 62 km^2. Measurements were made 300 m upstream of the confluence with the Gibbon River where Solfatara Creek flows in a 200 m wide grassy meadow below tree-covered slopes of glacial outwash. Channel banks are composed of medium to fine sand and silt and are capped by a grassy sod. The channel banks are generally steep to overhanging and are locally indented where the bank has collapsed.

The reach of channel investigated is a 20 m long, relatively straight section between two bends (Figure 1). Flow exits the upstream bend with the deepest portion of the channel along the left (outside) bank. With diminishing curvature, rapid shoaling develops, particularly along the left bank. Shoaling continues downstream to section 8 along the left bank and sections 9 and 10 near the centreline. Downstream of section 9 depth increases along each bank and the central bar tapers to a point between sections 10 and 11. Below section 11 flow depth becomes large across the entire channel. Air photos show that little channel migration has

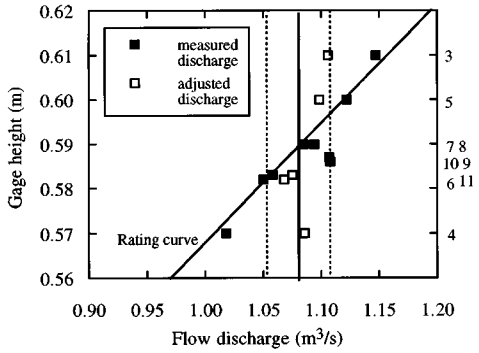

Figure 2. Rating curve (solid line) and collapse to common stage of 9·59 m for cross-sectional flow measurements. The filled squares represent the measured discharge and the open squares represent the adjusted-depth discharge. The dotted vertical lines are the bounds for 3 per cent error about the expected discharge of 1·08 $m^3 s^{-1}$. The numbers at the right refer to the cross-section

occurred in the study reach since the original photos of 1954, nor have major planform changes occurred along Solfatara Creek in the neighbourhood of the study reach.

The bed of Solfatara Creek is fine to medium gravel and coarse sand. The median size (D_{50}) is 8·0 mm, and D_{84} and D_{16} are 16·1 and 0·7 mm, respectively. Subscripts indicate the percentage that is finer. The largest grains are found along the left bank and over the central bar. The channel bed lacked bedforms and the gravel was immobile during measured flows. Sand moved in narrow corridors over the gravel bed and was deposited in a layer several centimetres thick along the inside bank at the downstream end of the upstream point bar and in the separated flow in the lee of the mid-channel bar front (downstream of sections 10 and 11). In areas not covered by the mobile sand, the surface was armoured. The ratio of the median grain size of the bed surface to that of the subsurface was 1·53.

The rating curve is shown in Figure 2. Bankfull discharge is estimated at 2.4 $m^3 s^{-1}$ from extrapolation of the rating curve and from the Manning equation assuming constant slope and roughness. In this paper the flow and local force balance are described for a stage of 9·59 m which corresponds to a discharge of 1·08 $m^3 s^{-1}$. The previous paper examined flow at a stage of 9·52 m which corresponds to a total discharge of 0·73 $m^3 s^{-1}$ (Whiting and Dietrich, 1991). These represent 45 and 30 per cent of the bankfull discharge, respectively.

METHODS

Field measurement

The topographic map (Figure 1) was made with a level and tape measure. In the channel, the water surface was used as a datum and measurements of the distance from the bed to the water surface were recorded and converted to elevation. Depth was measured at 0·2 m intervals across the channel, except close to the banks, and at about 0·7 m intervals along the channel. Stage did not vary by more than several millimetres during the depth measurements. The accuracy of the bed elevation is about 1 cm. From the map of the reach, the position of the channel centreline was defined and was used to compute the curvature of the channel trace.

Water surface topography was measured at 0·2 m intervals across the channel and at about 0·7 m intervals along the channel. All measurements were made from moveable bridges. A small nail was attached to the survey rod and when the nail just touched the water surface a reading with the level was taken. The reading was made three or more times until a consistent value was obtained. The accuracy is about 0·5 mm. Stage varied by 6 mm during the 4–5 h of measurement of the water surface topography. Frequent observations of the water level at a stage plate were used to adjust water surface measurements to a common stage. Water temperatures varied between 8 and 14°C.

Bed material was collected for grain-size analysis by scraping 200–300 g samples from the bed at 0·4–0·6 m intervals across the sections. Subsurface samples were obtained by a second scraping after the removal of the

surface particles. Samples of the bed were collected after flow measurements had been completed. Sediment samples were dried in the laboratory and sieved at half-phi intervals.

Impeller current meters suspended from a moveable wooden bridge were used to measure the flow. The current meters consist of a 3·5 cm diameter impeller housed in a 1·6 cm long, 4·2 cm diameter cage. (There is an illustration of the meters in Figure 5 of Whiting and Dietrich, 1991). A sensor notes a variation in the magnetic field caused by the rotation of small magnets in the impeller blades and a built-in timer records the number of revolutions which is then related to the flow velocity. The meters have an accuracy of ±0·3 cm s^{-1} or ±1·2 per cent, whichever is larger (Smith, 1978). Two pairs of meters were mounted 10 cm apart on a vertical support rod that was raised and lowered by a handcrank. In each pair, the meters were 10 cm apart, orthogonal, and facing upstream such that each meter was oriented 45° to the channel cross-section. The upper and lower pairs were 10 and 18 cm upstream of the axis of the support rod. Both sets of meters were below the base of the rod. The meters have a cosine response to flow that approaches the meters tangentially (Smith, 1978). This calibration for angle of attack was used to solve for the flow vector whose magnitude and orientation gave the observed readings on the orthogonal meters. At 0·2–0·4 m intervals across the sections shown on Figure 1, the stacked array of meters was lowered close to the bed and the flow measured for 200 s. The array was then raised in 2·5 cm increments and flow remeasured over the lowermost 20 cm of depth, and then raised by 5 cm steps. Downstream of steep bar fronts and near banks, flexible plastic flags were used to confirm the direction of flow determined from the meters. The meters were repeatedly observed through the clear flow to prevent fouling of the meters by organic material or bed material. Measurements of flow were made to within 0·10–0·25 m of each bank.

More information on methods is available in Whiting and Dietrich (1991).

Equations describing the flow

Smith and McLean (1984) expressed the governing equations for steady flow in a channel with varying curvature and topography in terms of an orthogonal, curvilinear coordinate system following the channel trace: *s* is parallel to the channel centreline, *n* is perpendicular to the centreline, and *z* is perpendicular to the hypothetically planar bed. The origin for *z* is the bed surface. The coordinates are positive downstream, toward the left bank, and upwards, respectively. The downstream, cross-stream, and vertical force balance equations and the continuity equation are written

$$(\tau_{zs})_b = -\frac{\rho g h}{(1-N)}\frac{\partial E}{\partial s} - \rho\frac{1}{(1-N)}\frac{\partial}{\partial s}\langle u_s^2\rangle h - \rho\frac{\partial}{\partial n}\langle u_s u_n\rangle h + 2\rho\frac{\langle u_s u_n\rangle h}{(1-N)R} \quad (1)$$

$$(\tau_{zn})_b = -\rho g h\frac{\partial E}{\partial n} - \rho\frac{\langle u_s^2\rangle h}{(1-N)R} - \rho\frac{1}{(1-N)}\frac{\partial}{\partial s}\langle u_s u_n\rangle h - \rho\frac{\partial}{\partial n}\langle u_n^2\rangle h + 2\rho\frac{\langle u_s^2\rangle h}{(1-N)R} \quad (2)$$

$$P_z = \rho g(h-z) \quad (3)$$

$$\frac{1}{1-N}\frac{\partial\langle u_s\rangle h}{\partial s} - \frac{\langle u_n\rangle h}{(1-N)R} + \frac{\partial\langle u_n\rangle h}{\partial n} = 0 \quad (4)$$

$(\tau_{zs})_b$ and $(\tau_{zn})_b$ are the downstream and cross-stream components of the boundary shear stress, ρ is the fluid density, *g* is the gravitational acceleration, *h* is the local flow depth, *E* is the water surface elevation, *u* is the flow velocity with the components in the *s*- and *n*-directions denoted by subscripts, and *P* is the pressure. *R* is the

centreline radius of curvature with its sign given by n, and N is transverse distance from the centreline divided by the radius of curvature. The term $1/(1\text{-}N)$ accounts for differential path length associated with transverse position. The angle brackets indicate that the quantity has been vertically averaged.

Equation 1 is the downstream balance between the boundary shear stress and the sum of the pressure gradient force, the change in momentum of the downstream flow in the streamwise direction, the change in downstream momentum in the cross-stream direction, and the force associated with the curvature. Equation 2 is the cross-stream balance between the boundary shear stress and the sum of the cross-stream pressure gradient force, the centrifugal acceleration (second and fifth terms to the right of the equal sign) and the change in cross-stream momentum in the downstream and cross-stream directions (third and fourth terms to the right of the equal sign). The vertical force balance reduces to the hydrostatic condition as presented in Equation 3 since the vertical velocity is small (Whiting and Dietrich, 1991).

These vertically averaged equations can be rewritten in terms of components of the downstream and cross-stream water surface slopes. The approximations have been made that $\langle u_s^2\rangle = \langle u_s\rangle\langle u_s\rangle$, $\langle u_n^2\rangle = \langle u_n\rangle\langle u_n\rangle$ and $\langle u_s u_n\rangle = \langle u_s\rangle\langle u_n\rangle$ (Dietrich and Smith, 1983).

$$S = \frac{(\tau_{zs})_b}{\rho g h} + \frac{\langle u_s\rangle}{g(1+N)}\frac{\partial\langle u_s\rangle}{\partial s} + \frac{\langle u_n\rangle}{g}\frac{\partial\langle u_s\rangle}{\partial n} - \frac{\langle u_s\rangle\langle u_n\rangle}{gR(1-N)} \tag{5}$$

$$S_n = -\frac{(\tau_{zn})_b}{\rho g h} - \frac{\langle u_s\rangle^2}{Rg(1-N)} - \frac{\langle u_s\rangle}{(1\text{-}N)g}\frac{\partial\langle u_n\rangle}{\partial s} - \frac{\langle u_n\rangle}{g}\frac{\partial\langle u_n\rangle}{\partial n} \tag{6}$$

For simplicity in the ensuing discussion, Equations 5 and 6 are rewritten to assign each term a label and $S = [1/(1–N)]\, dE/ds$ and $S_n = dE/dn$:

$$S = S_1 + S_2 + S_{3a} + S_{3b} \tag{7}$$

$$S_n = S_{n1} + S_{n2} + S_{n3} + S_{n4} \tag{8}$$

The total boundary shear stress in the downstream and cross-stream directions is estimated by approximating the drag as:

$$S_1 = \frac{C_d}{2gh}\cos\beta\left[\langle u_s\rangle^2 + \langle u_n\rangle^2\right] \tag{9}$$

$$S_{n1} = \frac{C_d}{2gh}\sin\beta\left[\langle u_s\rangle^2 + \langle u_n\rangle^2\right] \tag{10}$$

where β is the near-bed flow direction. The drag coefficient (C_d), calculated by the assumption of uniform downstream flow over many channel widths, has a value of 0·0462. Bedforms are lacking so the bulk of the total boundary shear stress reflects the resistance of the bed and irregular banks and variation in width. The formulation of S_{nl} explicitly defines the stress direction to be parallel to the near-bed flow direction and in this way incorporates the effect of secondary flow. The two equations above were incorrectly written in the text of Whiting and Dietrich (1991). The results were not affected by this typographical error.

Section orientation

The appropriate cross-section orientation is critical in the determination of the force balance because it defines the cross-stream and downstream components of flow. The approach used herein is from Dietrich and Smith (1983). Sections are oriented in the field to be perpendicular to the banks, and flow measurements are

made along these sections. The flow measurements and the continuity equation are then used to calculate the local cross-stream flux required to account for the differences in the downstream velocity field between sections upstream and downstream of the section under consideration. These calculated local cross-stream fluxes, when integrated across the channel, give the cross-stream discharge for the section from continuity, $Q_{nw,c}$. By comparing this value to the cross-stream discharge from the measured local $\langle u_n \rangle$ values, $Q_{nw,m}$, the required angular reorientation of the section, θ_w, is calculated. Q_{sw} is the downstream flow discharge.

$$Q_{nw,c} = \int_{-w/2}^{w/2} \left(\frac{-1}{1-N} \int_{-w/2}^{n} \frac{\partial \langle u_s \rangle h}{\partial s} \, dn \right) dn \tag{11}$$

$$Q_{nw,m} = \int_{w/2}^{w/2} \langle u_n \rangle h \, dn \tag{12}$$

$$\theta_w = \tan^{-1} \left(\frac{Q_{nw}}{Q_{sw}} \right) \tag{13}$$

Discharge collapse

Section orientation based on cross-stream integration of differences in the downstream discharge is predicated upon equal discharge between sections. Differences in measured discharge between sections can arise from the real non-uniformity of stage and the apparent variation stemming from the assumptions used to extrapolate velocities to the bed, bank and water surface. At Solfatara Creek, stage varied by about 0·4 cm and never by more than 1·0 cm during the 8–10 h period typically required to measure flow across a single section. Day-to-day stage variation was larger and due to precipitation and diminishing snowmelt. The results presented in this paper are for a common stage of 9·59 m which corresponds to a discharge of 1·08 $m^3 s^{-1}$. Because of the fluctuations in discharge from day to day, adjustment of the measured discharge to the common stage and discharge was necessary in some cases. It was found that most of the difference in discharge could be accounted for by the difference in depth between the measured stage and the common stage of 9·59 m (Figure 2). Vertically averaged velocity was held constant during this slight modification in depth. Using this method, the discharge variation about the common stage averaged 1·5 per cent. These small differences were then accounted for by normalizing the vertically averaged velocities by the ratio of expected total discharge to the recalculated measured discharge. At other sections, the stage during measurement was 9·59 m and so no adjustment was necessary.

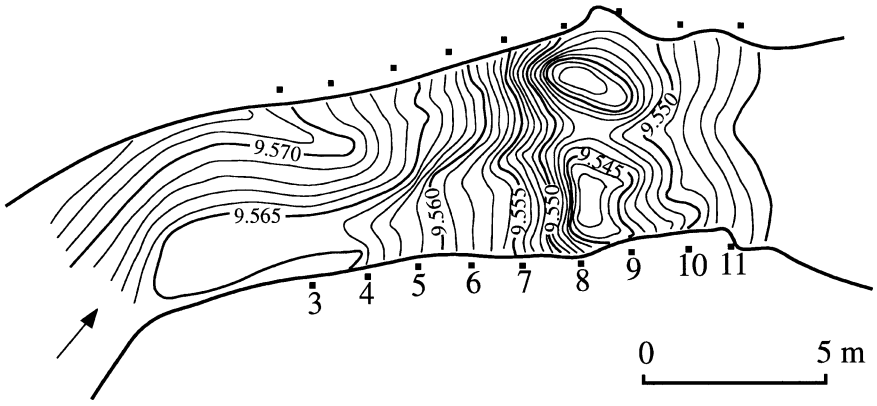

Figure 3. Water surface elevations at a stage of 9·57 m. The contour interval is 1 mm

The normalized vertically averaged velocities were located in the section with respect to the channel centreline as digitized from the planform map. These values were then used with the continuity equations (11, 12 and 13) to determine the realignment required by continuity. The realignment of sections required for continuity averaged 3·0°. Further recalculation and reorientation was unnecessary.

WATER SURFACE TOPOGRAPHY AND FLOW FIELDS

The water surface topography at a stage of 9·57 m is shown in Figure 3. At the exit of the upstream bend the water surface is higher along the outer (left) bank associated with superelevation. The downstream water surface slope coming out of the bend is relatively weak. Downstream of section 4, the water surface elevations drop more rapidly, especially along the left bank, such that by section 7 the water surface across the channel is at about the same elevation. There are important local variations across the section, however. The water surface continues to drop downstream of section 7 to about halfway between sections 8 and 9. Two local water surface lows are found flanking the edge of the bar between sections 8 and 9. Downstream of section 9, the water surface climbs in elevation in deepening and decelerating flow. The pattern of water surface elevations in Figure 3 is grossly similar to that shown in Whiting and Dietrich (1991) at a lower stage. One major difference between the stages is the magnitude of the transverse water surface slope in the upstream bend. At the higher stage described here, the magnitude of the superelevation is greater and the superelevation persists for a longer distance downstream. Another difference is that the downstream water slope is more uniform at the higher stage and the cross-stream slope upstream of the bar top is only about half as steep as at the lower stage.

The downstream and cross-stream flow fields for a stage of 9·59 m are shown in Figure 4. The largest streamwise velocities are to the left of the channel centreline at sections 3 and 4 as a consequence of the cross-over in the upstream bend. At sections 5 and 6 streamwise flow velocity increases and the highest downstream velocities are over the shallowest part of the section. From sections 6 to 8 the flow continues to accelerate and the largest downstream flow velocities are approximately in the middle of the channel over the topographic high. At section 9, the highest velocities are not appreciably greater than at section 8. At section 10, flow has bifurcated into two strands of high streamwise velocity along each side of the wedge-shaped bar front. Near-bed flow slows dramatically.

The cross-stream flow pattern at the upper cross-section (cross-section 3) is towards the left bank (outward) near the surface, while near-bed flow is towards the right bank (inward) (Figure 4). By section 4, flow is towards the right bank in most parts of the section. At section 5, cross-stream flow is towards the right bank in much of the channel, but flow towards the left bank develops to the left of the centreline. Flow towards the right bank continues to strengthen at section 5. Downstream of sections 5 to 7, flow remains directed towards the right bank over the shallowest areas, but is not quite as strong. At section 8, flow to the right of the shallowest part of the bar is towards the right bank whereas to the left of the bar top, flow is towards the left bank. At sections 9 and 10 surface flow is away from the bar top towards the banks while flows near the bed are towards the crest of the bar. This creates two opposing spirals. At section 10, where flow deepens dramatically, velocities decrease, especially near the bed. Downstream of section 10, flow separated at the lower stage.

Figure 5 presents a comparison of the vertically averaged downstream flow velocity at the two stages. The values shown have been linearly interpolated from the measured velocity to the velocity expected at the 25 cm spacing used in the calculations. The values shown are those used in the calculations. In general, the flow pattern at the higher stage is fairly similar to that observed at the lower stage (Whiting and Dietrich, 1991), but downstream flow velocity is larger at the higher stage. The transverse variation in the magnitude of the downstream flow is reduced at sections 8 and 9 at the higher stage. In this region the flow is shallow (Figures 1 and 4) and the bed is coarser than in most other areas. It appears that local variations in the flow associated with the topography and large grains are being ‘drowned out’ at this slightly higher stage. At section 10, the jet of higher flows is further away from the right bank at the higher stage.

Figure 6 compares the vertically averaged cross-stream flow velocity at the two stages. The patterns are grossly similar, but the absolute value of the cross-stream flow velocity is generally less at the higher stage,

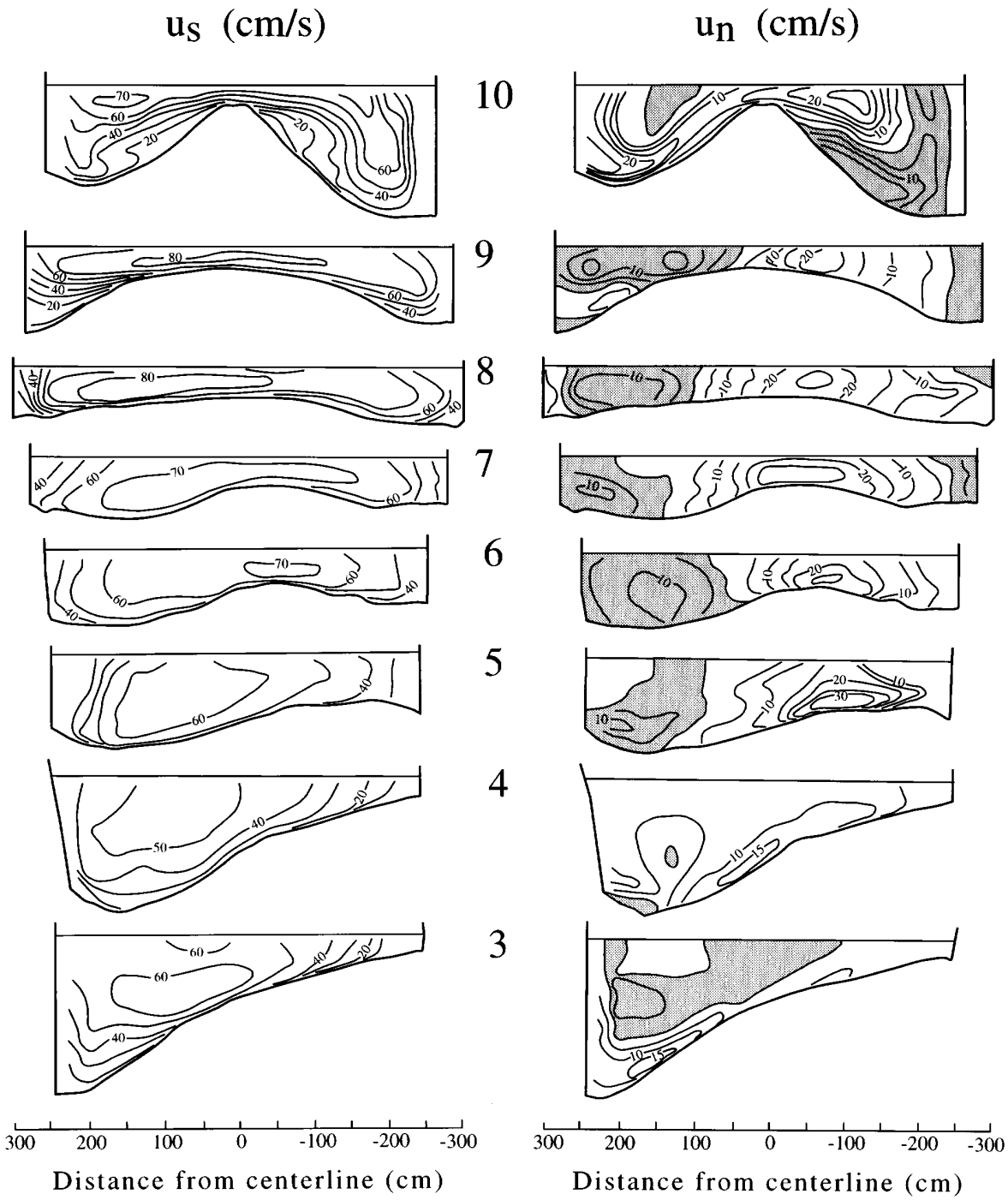

Figure 4. Downstream (u_s) and cross-stream (u_n) velocity fields at sections. These values have been reoriented to conform with continuity and normalized to the common stage. Shaded areas in the cross-stream panel indicate positive values (flow toward the left bank)

except near the left bank at sections 5 to 8. The decrease in the absolute value of the deviations from the downstream direction is particularly true in the middle of the study reach (sections 5 to 8) where flow is the shallowest. Since the downstream flow velocity at the higher stage is larger (Figure 5), and the cross-stream velocities are generally less, the flow more closely parallels the downstream direction at the higher stage. For

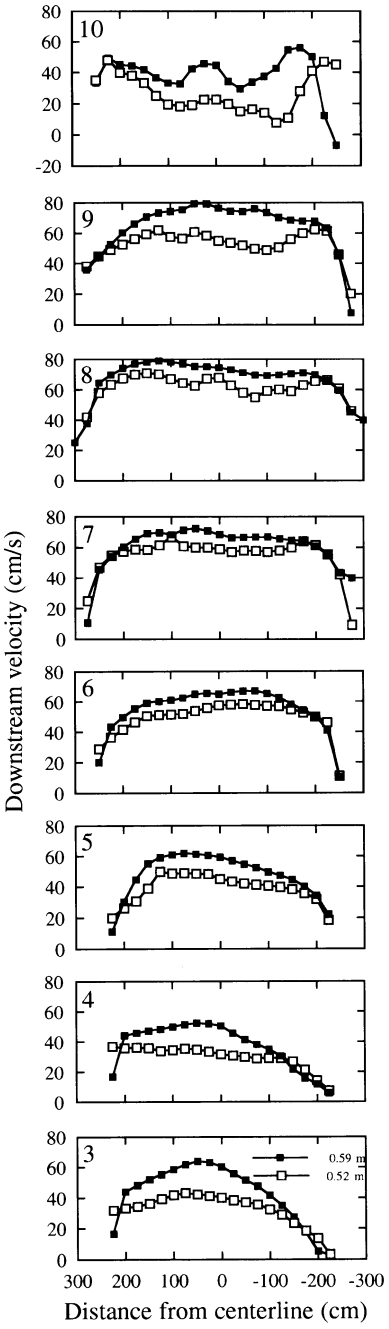

Figure 5. A comparison of interpolated vertically averaged downstream velocity $\langle u_s \rangle$ at the two stages, 0·52 m and 0·59 m

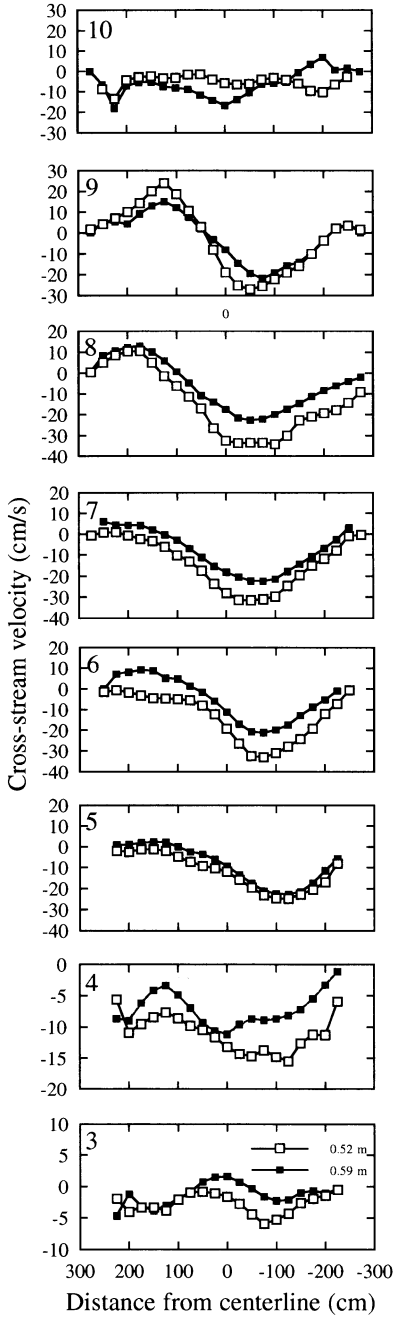

Figure 6. A comparison of interpolated vertically averaged cross-stream velocity $\langle u_n \rangle$ at the two stages, 0·52 m and 0·59 m. Note the ordinate scale change between sections 4 and 5

example, 1m to the right of the centreline at section 7, the flow deviates from the *s*-direction by 20° while at the same location at the lower stage the flow deviates by 28°. In both cases the flow is towards the right bank. At section 10, the magnitude of the cross-stream flows is as large as at the lower stage. The variation in flow direction at the different stages is distinct and cannot be ascribed to section orientation.

COMPONENTS OF THE FORCE BALANCE

Figure 7 compares the predicted and observed downstream water surface slopes at each section. These predicted slopes were calculated from Equations 6, 7 and 8. The observed downstream slopes at sections were computed from the map of water surface elevations over distances of 1·0 m (Figure 3). The pattern of water surface slopes at the stage for which calculations were done (9·59 m) is assumed to be unchanged from the pattern observed during measurement at a stage of 9·57 m. The equations predict correctly the weak downstream water surface slope in upstream sections (4 and 5) and the subsequent steepening over the bar (sections 6, 7 and 8). Also predicted is the adverse water surface slope flanking the central bar at section 9, although the measured slope over the middle of the bar is much less than the predicted slope. At section 10, both predicted and observed slopes are negative, indicating an adverse pressure gradient. The results are similar to those reported in Whiting and Dietrich (1991) for the lower stage.

The ability to predict the observed streamwise water surface slope depends upon both the proper incorporation of all the important terms in the governing equations as well as the ability to calculate these terms correctly. The largest uncertainty may be associated with the measured slope value. Figure 8 plots the components of the downstream slope at each section. Components S_1 and S_2, the shear stress term and downstream acceleration term, are important throughout the reach. S_{3a}, which represents the cross-stream transport of downstream momentum, is generally smaller than either S_1 or S_2, but commonly determines the structure of the slope variation across the section. S_{3b} is small because of the overall straightness of the channel and is not shown. The relative importance of the different terms is similar to that at the lower stage (Whiting and Dietrich, 1991), but the cross-stream transport of downstream momentum S_{3a} is generally lower at the higher stage. This follows from the observation that cross-stream velocity is not as great at the higher stage (Figure 6). S_2, the downstream transport of downstream momentum, is very comparable in structure at the two stages, although the magnitude of S_2 is slightly greater at the higher stage (*c.* 20 per cent higher). S_2 (proportional to $<u_s>\partial<u_s>/\partial s$) is larger at the higher stage because downstream velocity is greater (Figure 5). S_1, the shear stress term, is generally similar at the two stages. While the velocity is greater at the higher stage, this is somewhat compensated for by the increase in depth, particularly over the bar top.

The observed and predicted cross-stream water surface slope are shown in Figure 9. The components of the cross-stream slope are shown in Figure 10. The observed local slope was calculated from the water surface elevation difference over a transverse distance of 0·5. The calculations are able to reproduce the transverse slope that is tilted towards the right bank in the upstream sections. Also reproduced faithfully is the rapid decay of this cross-stream tilt along the right bank at section 8 and the rapid development of a cross-stream tilt towards the right bank to the right of the central bar. The cross-stream slope pattern is not predicted well at section 10, where flow deepens dramatically.

The centrifugal term, S_{n2}, important only at upstream sections where curvature is significant, is not shown in the chart of the components of the cross-stream force balance (Figure 10). S_{nl}, the effect of the transverse component of the boundary shear stress, is largest from sections 6 to 9, but it is not as important here as at the lower stage. This term is less important because, while the flow is faster, the angle the flow makes with the downstream direction is less and the depth is greater. S_{n3} and S_{n4}, as at the lower stage, are the largest terms. These terms account for the effects that the downstream and cross-stream transport of cross-stream momentum have on the transverse slope. Of the two terms, S_{n3} is the least affected by the difference in stage. S_{n4} is generally less important at the higher stage because in much of the channel the absolute value of the vertically averaged cross-stream velocity is less, and because the magnitude of its transverse variation is less (Figure 6).

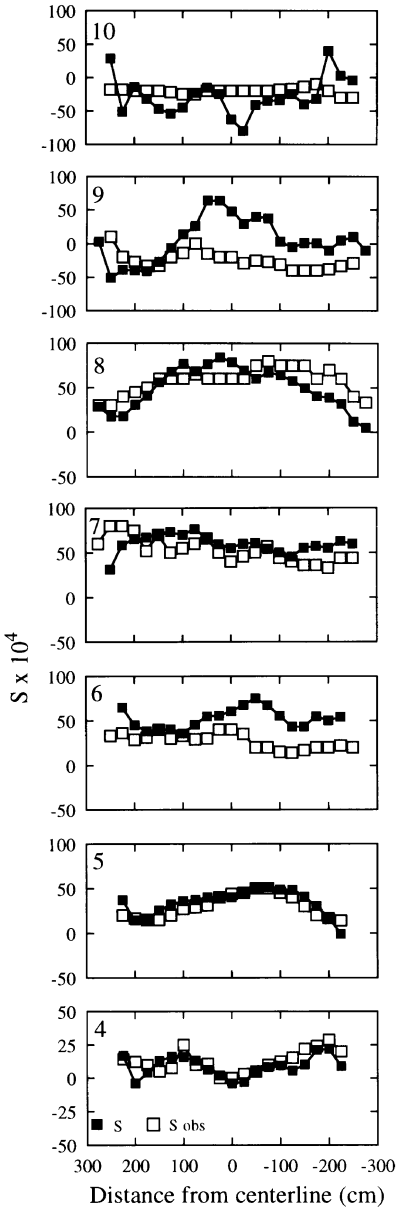

Figure 7. Observed and predicted downstream water surface slope. Note the ordinate scale change between sections 4 and 5 and between sections 8 and 9

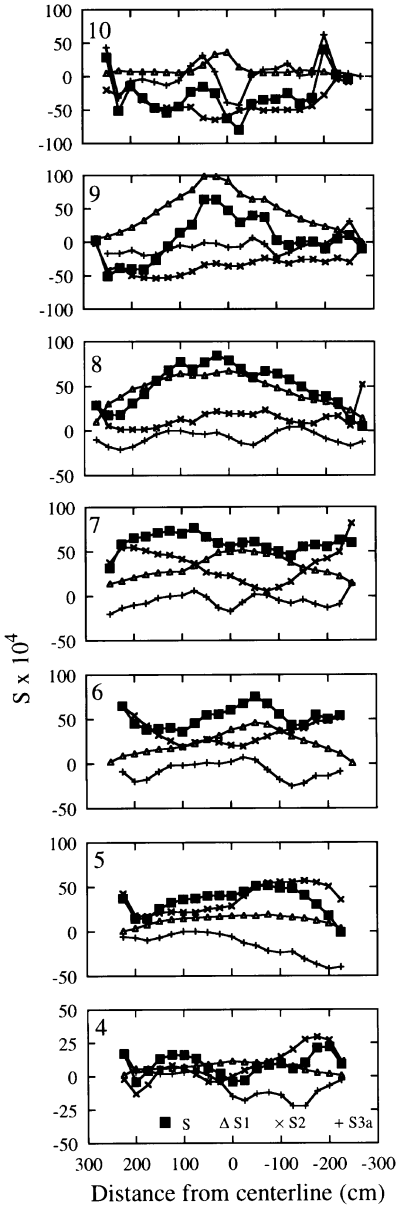

Figure 8. Components of the downstream force balance. Note the ordinate scale change between sections 4 and 5 and between sections 8 and 9

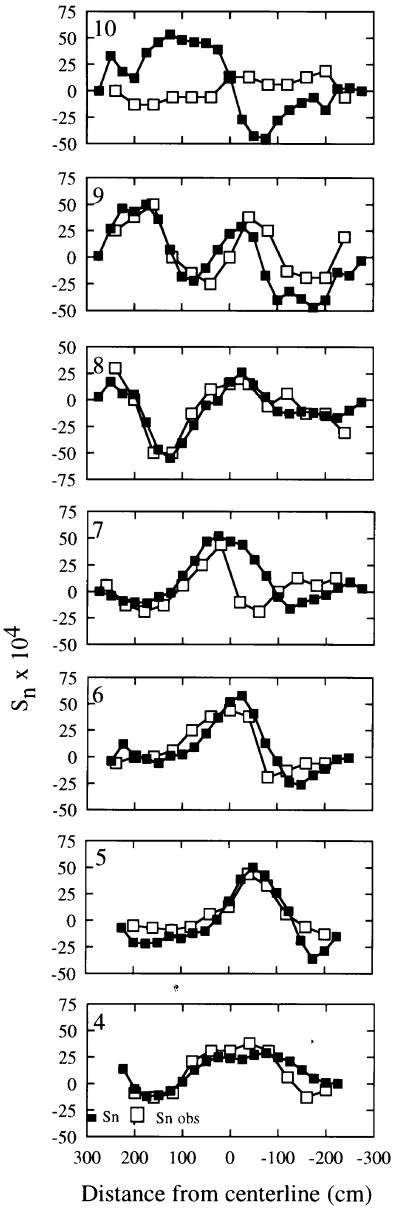

Figure 9. Observed and predicted cross-stream water surface slope

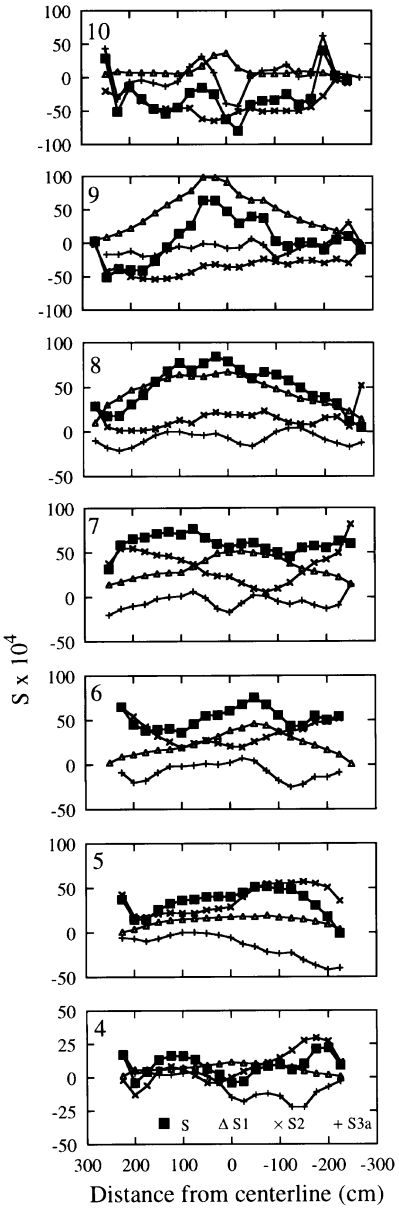

Figure 10. Components of the cross-stream force balance. S_{n2} was not included because it was small

DISCUSSION

The results from both stages taken together reaffirm the importance of the convective accelerations in the governing equations (Yen and Yen, 1971; Dietrich and Smith, 1983; Dietrich and Whiting, 1989), particularly in the absence of significant curvature. However, a comparison of the results at Solfatara Creek for the different stages indicates that the terms associated with lateral flow (S_{nl}) and lateral momentum fluxes (S_{3a}, S_{n4}) decrease in importance as the stage rises. This can be explained by the progressively deeper flow over the central bar. At lower flows, the water spills over the edge of the bar and bifurcates as it goes around both sides of the bar. At higher stages the flow goes more nearly over the bar and deflection of the flow toward the bank is less. As the flow is more directly downstream, cross-stream velocity is reduced and those terms associated with transverse momentum fluxes are reduced.

Various workers have reached differing conclusions regarding the importance of the components of the force balance. Most of these studies have been for flow around bends (Dietrich and Smith, 1983; Odgaard and Bergs, 1988; Dietrich and Whiting, 1989). There is a general consensus that terms S_1 and S_2 must be included in the downstream force balance. Yen and Yen (1971) and Dietrich and Smith (1983) have argued that cross-stream transport of streamwise momentum (S_3) must be included as well. Odgaard and Bergs (1988), on the other hand, found that the cross-stream transport of downstream momentum (S_{3a} in this paper) was not important. Engelund (1974) did not include this term in his model. Less attention has been focused on the cross-stream force balance. Odgaard and Bergs (1988) found that S_{n2} was the most important, with S_{n3} and S_{nl} being of lesser importance. Dietrich and Whiting (1989) found that in Muddy Creek the terms S_{n3} and S_{n4} were usually smaller than S_{n2}.

Some of the difference in results from different workers may be ascribed to differences in the magnitude of topographic variation in a manner that is similar to the relative importance of terms at Solfatara Creek as stage changes. The topographic relief might be described by ratio of the local maximum depth to the average depth. When topographic relief is smaller, the terms associated with topographic forcing are less important. Odgaard and Bergs (1988) found that the cross-stream transport of downstream momentum term (S_{3a} in this paper) was not important. In their flume study, topographic relief was 1·8. Bridge and Gabel (1992) also felt that this term was of minor importance. Topographic relief was 2·0. Dietrich and Smith (1983) found that S_{3a} was often opposite in sign to S_{3b} and had to be included, even though its local value was minor in some areas. Topographic relief was about 1·8. At Solfatara Creek, topographic relief was 2·25 and 2·10 at the lower and higher stages, respectively. At both stages, the cross-stream transport of downstream momentum term was important to the overall force balance. Consistent with these results from the other sites is that the convective acceleration term is more important in streams with stronger topographic forcing; the Solfatara case with the lower topographic relief is a case when the relative importance of S_{3a} is less.

CONCLUSION

The flow and shear stress fields at the two stages at Solfatara Creek show that convective acceleration terms in the equations governing flow in a channel reach are important. A comparison of the relative importance of these terms indicates that those terms associated with lateral flow and lateral momentum fluxes become less important as the stage rises and topographic forcing of flow is reduced. That is not to say that these terms become unimportant at higher stages. Particularly where there are rapid changes in depth, or bed or bank roughness, the inclusion of these terms is probably essential for a reasonable estimate of the boundary shear stress pattern. Furthermore, since these areas are often at critical locations in a channel, such as the edge of the bar and the tail of the pool, inclusion of these terms is necessary to predict important features of the channel. Part of the explanation for the different findings on the importance of convective acceleration terms in the force balance may be due to the magnitude of the topographic relief in each study.

ACKNOWLEDGEMENTS

George Ehlers assisted in the field work. I thank the superintendent and research staff of Yellowstone National Park for permission to work in the park and for their cooperation during the study. John Bridge, Jon Nelson and two anonymous reviewers improved earlier drafts of this manuscript. Acknowledgement is made to the Donors of The Petroleum Research Fund administered by the American Chemical Society for support of this research (ACS-PRF-18427-AC2).

REFERENCES

Bridge, J. S. and Gabel, S. L. 1992. 'Flow and sediment dynamics in a low sinuosity, braided river: Calamus River, Nebraska Sandhills', *Sedimentology*, **39**, 125–142.

Dietrich, W. E. and Smith, J. D. 1983. 'Influence of the point bar on flow through curved channels', *Water Resources Research*, **19**, 1173–1192.

Dietrich, W. E. and Whiting, P. J. 1989. 'Boundary shear stress and sediment transport in river meanders of sand and gravel', in Ikeda, S. and Parker, G. (Eds), *River Meandering*, American Geophysical Union Water Resources Monograph **12**, 1–50.

Dietrich, W. E., Smith, J. D. and Dunne, T. 1984. 'Boundary shear stress, sediment transport and bed morphology in a sand-bedded river meander during high and low flow', in Elliot, C. M. (Ed.), *River Meandering: Proceedings of the Conference, Rivers '83*, American Society of Civil Engineers, New York, 632–639.

Engelund, F. 1974. 'Flow and bed topography in channel bends', *Journal of the Hydraulics Division, ASCE*, **100**, 1631–1648.

Jackson, R. G. 1975. 'Velocity–bedform–texture patterns of meander bends in the lower Wabash River of Illinois and Indiana', *Geological Society of America Bulletin*, **86**, 1511–1522.

Odgaard, A. J. and Bergs, M. A. 1988. 'Flow processes in a curved alluvial channel', *Water Resources Research*, **24**, 45–56.

Rhoads, B. L. and Kenworthy, S. T. 1995. 'Flow structure at an asymmetrical stream confluence', *Geomorphology*, **11**, 273–293.

Smith, J. D. 1978. 'Measurement of turbulence in ocean boundary layers', paper presented at *Working Conference on Current Measurement*, Office of Ocean Engineering, National Oceanic and Atmospheric Administration, University of Delaware, Newark, DE, 11–13 Jan. 1978, 95–128.

Smith, J. D. and McLean, S. R. 1984. 'A model for meandering rivers', *Water Resources Research*, **20**, 1301–1315.

Whiting, P. J. and Dietrich, W. E. 1991. 'Convective accelerations and boundary shear stress over a channel bar', *Water Resources Research*, **27**, 783–796.

Yen, C. L. and Yen, B. C. 1971. 'Water surface configuration in channel bends', *Journal of the Hydraulics Division, ASCE*, **97**, 303–321.